Front. Chem. China 2010, 5(1): 61–70
DOI 10.1007/s11458-009-0099-3

FEATURE ARTICLE

Recent advances in strontium tungstate scheelite material

Aixiang WANG (✉)[1], Cuifang WANG[2] and Guohua JIA (✉)[3]

1 College of Chemistry and Chemical Engineering, Linyi Normal University, Linyi, Shandong 276000, China
2 College of Chemistry and Chemical Engineering, Fuzhou University, Fuzhou, Fujian 350002, China
3 Department of Biology and Chemistry, City University of Hong Kong, Kowloon, Hong Kong, China

Strontium tungstate is a well-known stimulated Raman scattering laser material. The unique structure of this crystal allows the usage of these crystals as matrices for laser active elements with nonlinear self-conversion of radiation to a new spectral range. The recent advances in crystal growth, particle and thin film fabrication, spectroscopy, and laser properties were reviewed. The demonstration of laser output of neat and Nd^{3+}-doped $SrWO_4$ crystal shows that it is an efficient self-stimulated Raman scattering laser.

Keywords $SrWO_4$, spectroscopic property, stimulated Raman scattering, laser crystal

1 Introduction

Recently, there has been burgeoning interests in the study of strontium tungstate scheelite material because of its large transparent spectral range, suitable hardness, and the unique nonlinear optical property, namely, stimulated Raman scattering. Stimulated Raman scattering is a promising new method to produce new laser emission wavelengths; this effect is owned to the structure of the material. By employing the material as the matrix, one can combine the laser active elements, e.g. lanthanide ions, with the stimulated Raman scattering effect to generate laser radiation into new spectral ranges.

In this feature article, we will review recent works on the synthesis, characterizations of optical spectroscopy, and laser properties of the tungstate scheelite materials. An emphasis will be put on the demonstrations of the stimulated Raman scattering, which serves as an insight into the application of this material in new spectral ranges.

2 Crystal structure

Strontium tungstate crystallizes in a tetrahedral structure in the space group of C_{4h}^6 ($I4_1/a$), space no. 88, with 4 molecules in each crystallographic unit [1–3] at atmospheric pressure. The strontium atoms accommodate on the 4b Wyckoff site with an S_4 symmetry. This compound undergoes a phase transition from scheelite to fergusonite with the ambient pressure at about 10×10^9 Pa [2–5] (Figure 1). The strontium tungstate fergusonite belongs to the C_{2h}^6 ($C2/c$), space no. 15, with also 4 molecules in each crystallographic unit [2–5]. The site symmetry of strontium atoms is C_2, which is much lower than in the scheelite structure.

Received September 2, 2009; accepted October 19, 2009
E-mail: wangaixiang1974@163.com, ghjia@hotmail.com

3 Synthesis

3.1 Bulk crystal growth

Packter and Roy [6] have described the crystallization of strontium tungstate from the melted lithium chloride solution at low temperature. In this case, crystals can only grow into the sizes of several centimeters because of its limited solubility in the melt. Since strontium tungstate melts congruently and there is no phase transition in the temperature range from ambient to the melting point at atmospheric pressure, it can be grown into sizes of centimeters by the Czochralski method. Contrary to the traditional solvent-growth method, this method is easy to control and does not involve the complicated procedure in which types of solvent are varied and portions of each solvent are adjusted.

Neat and rare-earth ions doped strontium tungstate crystals were grown by the Czochralski method [7–9]. Chemicals were used as received without further purification. $SrCO_3$ (AR), WO_3 (AR), and Ln_2O_3 (Ln = Nd,Tm,Er,Yb,Pr)

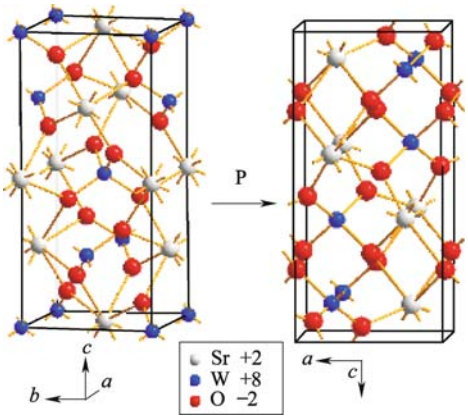

Figure 1 Scheelite (left) and fergusonite (right) structures of strontium tungstate.

(99.99%) were mixed separately in the molar ratio in an agate motor. The mixture was pressed into plates and then transferred into a platinum crucible. The crucible was heated to 1100°C and was kept at this temperature for one week. Then the chemicals were deposited in an iridium crucible and were placed in the DJL-400 furnace under nitrogen atmosphere. The mixture was heated to a temperature of 50°C higher than the crystallization temperature for about 2 h to allow the melt to mix completely and homogeneously. Neat $SrWO_4$ seed was selected from small crystals obtained by spontaneous crystallization and was used to grow bulky $SrWO_4$ crystal. The seeds used in the subsequent experiments were oriented parallel to the *c*-axis. The rotate and pulling rates were 12–15 rpm and 1–1.2 mm·h^{-1}, respectively. When these procedures were over, the crystals were drawn out of the melt and cooled down to room temperature at a rate of 12–30°C·h^{-1}. The as-grown crystals containing different rare-earth ions show different colors (Figure 2), and the properties of each crystal are depicted in Table 1.

Table 1 Size, color, and segregation coefficient of the as-grown crystals

crystal	color	ion concentration (10^{19} cm^{-3})	segregation coefficient (%)
neat	colorless	–	–
Nd	sky-blue	8.5	20.09
Tm	colorless	6.2	15.78
Er	red	8.0	20.28
Yb	blue	3.85	9.80
Pr	green	20.9	49.40

It is important to note that some extra WO_3 should be added to the starting materials in order to compensate the loss of sublimation during the crystal growth. Similar phenomenon has also been observed in the growth of $La_2(WO_4)_3$ and

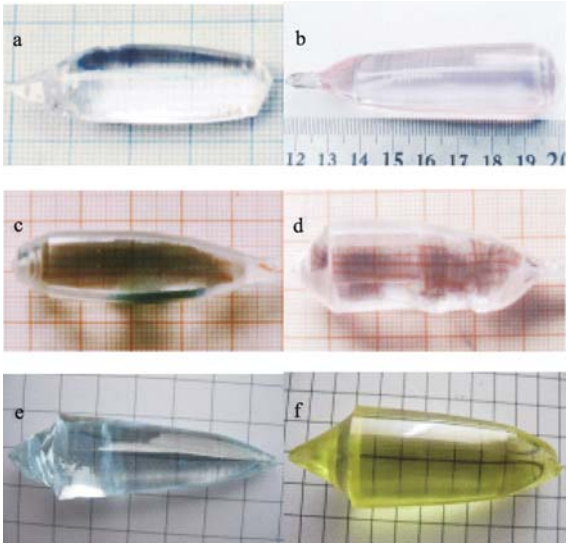

Figure 2 The photos of the as-grown tungstate strontium crystals: a. neat; b. Nd^{3+}; c. Tm^{3+}; d. Er^{3+}; e. Yb^{3+}; f. Pr^{3+}. Pictures are reproduced from Ref. [7].

$Sm_2(WO_4)_3$ crystals [6,10]. The addition of extra WO_3 ensures to balance the stoichimetric ratios of the starting materials.

3.2 Particle

The methods to fabricate strontium tungstate particles can be generally categorized into two types: one is a liquid-solution routine [11–22], the other is a molten flux process [23]. With the control of preparation conditions, the morphology of strontium tungstate particles is easy to be fabricated into peach-like, dump-like, bundle, rice grain-like, peanut-like, and rod-like particles (Figure 3). The synthesis of strontium tungstate particles involves the dissolution of the starting materials in water or some certain solvents and subsequently the treatment of as-prepared particle under microwave irradiation. In this way, fine, uniform particles with a narrow distribution can be successfully obtained.

3.3 Film

Strontium tungstate film can be prepared by a chemical solution method [24–30] (e.g. polymeric precursor and adjustable galvanic cell) by pulsed-laser deposition method [28], or by a spray pyrolysis method [29]. Figure 4 shows the scanning electron microscope (SEM) images with oxidant for 60 h and without oxidant for 80 h. The chemical solution method has been proved to be an inexpensive and environmentally friendly route for the preparation of strontium tungstate film.

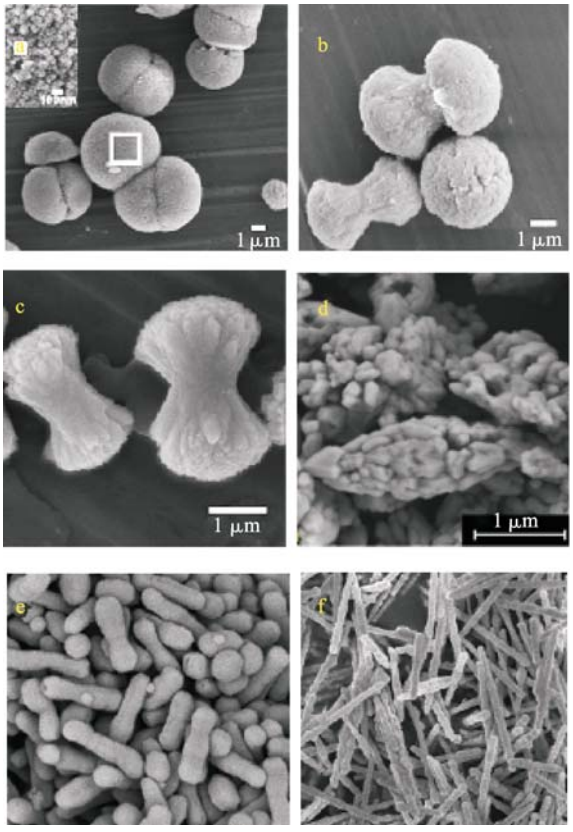

Figure 3 SEM images of $SrWO_4$. a. Peach-like; b. dump-like; c. bundle; d. rice grain-like; e. peanut-like; and f. rod-like. Figure reproduced from Refs. [11,20,22].

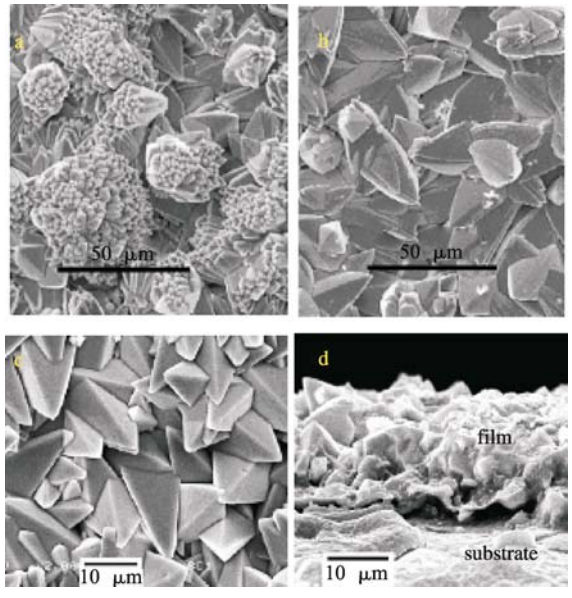

Figure 4 SEM images of $SrWO_4$ films prepared by galvanic cell method. a and b: in the presence of oxidant for 60 h; c and d: in the absence of oxidant for 80 h. Figure reproduced from Ref. [28].

4 Physical property

4.1 Thermal expansion

The measurements of thermal expansion have greatly increased our knowledge of material properties such as lattice dynamics, electronic and magnetic interactions, thermal defects, and phase transitions [31]. As a significant part of the power pump is converted into heat inside the material during laser operation, it is important to know its linear thermal expansion coefficients to predict how the material behaves when the temperature increases [32]. The figure of the linear expansions versus temperature was shown in Figure 5. The linear thermal expansion coefficient is defined as:

$$\alpha = \frac{1}{L}\frac{\Delta L}{\Delta T}, \tag{1}$$

where L is the initial length of the sample at room temperature, and ΔL is the change in length when the temperature changes ΔT. We can calculate the thermal expansion coefficient from the slope of the linear fitting of the linear relationship between $\Delta T/T$ and the temperature. In this case, the linear thermal expansion coefficients for different crystallographic direction c-, b-, and a-axes are 2.73×10^{-5}°C^{-1}, 1.00×10^{-5}°C^{-1}, and 1.05×10^{-5}°C^{-1}, respectively.

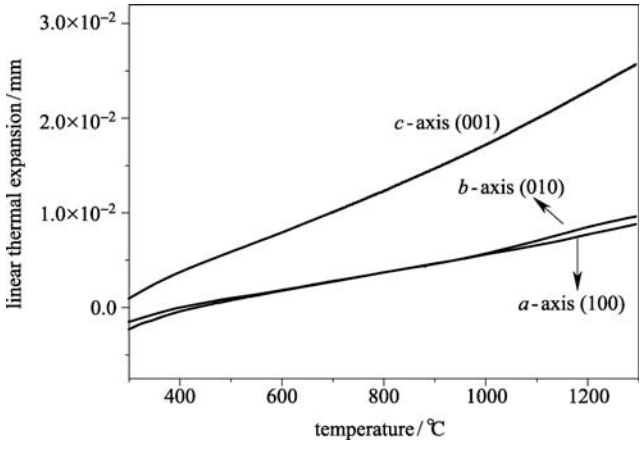

Figure 5 Linear thermal expansion coefficients of (001), (100) and (010) directions.

The thermal properties perpendicular to the crystallographic axes are theoretically equivalent in the uniaxial scheelite structure strontium tungstate crystal. The values of thermal expansion along a- and b-axes are comparable. The small difference of the values of thermal expansion between a- and b-axes thermal expansion can be attributed to experimental errors.

4.2 Refractive index

The minimum deviation technique with a prism sample is a popular method used in the refractive index measurements [33]. To fully characterize $SrWO_4$ crystal in terms of refractive indices as a function of wavelength, we have measured them with a precision of 1×10^{-4} at several different wavelengths from the visible to the near infrared. These data were fitted by the least-square method according to the Sellmeir equation [34]:

$$n_i^2 = \mathrm{A} + \frac{\mathrm{b}}{\lambda^2 - \mathrm{C}} - \mathrm{D}\lambda^2 \quad (2)$$

where λ is the wavelength, and A, b, C, and D are the Sellmeir parameters. By fitting the obtained data, we obtain the following equations (λ is in the unit of μm):

$$n_o^2 = 3.4383 + \frac{0.0523}{\lambda^2 + 0.001523} + 0.0049856\lambda^2 \quad (3)$$

$$n_e^2 = 3.4033 + \frac{0.0526}{\lambda^2 + 0.009456} + 0.0096059\lambda^2 \quad (4)$$

where n_o and n_e are the refractive indices for polarization perpendicular (ordinary) and parallel (extraordinary) to the axis of anisotropy, respectively. The measured and calculated refractive indices of $SrWO_4$ crystal were presented in Table 2. The curves obtained from the fit according to the Sellmeir equation are shown in Figure 6.

Table 2 Measured and calculated refractive indices of $SrWO_4$ crystal

λ(μm)	n_o	n_e
0.8080	1.87649	1.8678
0.6563	1.88701	1.87762
0.6328	1.88966	1.88072
0.5893	1.89472	1.88525
0.5780	1.89610	1.88669
0.5461	1.90077	1.89113
0.5321	1.90328	1.89298
0.4861	1.91294	1.90228
0.4358	1.92666	1.91574

5 Optical spectroscopy

5.1 Neat strontium tungstate

The luminescence of strontium tungstate has attracted extensive attentions in the past several decades [16,17,21,28,29,35–59]. It is generally assumed that the emission and excitation spectra of neat $SrWO_4$ are associated with the charge transfer within the WO_4^{2-} group [60]. The molecular orbital calculation for WO_4^{2-} group with the T_d symmetry group has been performed by Butler [61]. He pointed out that the ground and four singlet excited states predicted by crystal field approximation were $^1A_1$ and ^1A ($^1T_1$), $^1E(^1T_1)$, $^1E(^1T_2)$, and $^1B(^1T_2)$, respectively. The blue emission band has been attributed to an intrinsic emission associated with an electron transition from $^1B(^1T_2)$ to the ground state $^1A_1$ of WO_4^{2-} group. However, there is a controversy on the origin of the green emission (Figure 7). Some early work [37,39,40,43] attributed the green emission to (WO_3+ F) center in $PbWO_4$ single crystals, whereas Sokolenko et al. [42] and Sinelnikov [41] and coworkers assigned this emission to (WO_3+ Vacancy) oxygen-deficient complexes. Other authors [44–47] attributed the green emission to the defect centers with interstitial oxygen. So even though the photoluminescence of neat strontium tungstate crystal has been extensively studied, there are still issues in debate regarding the origin of the color centers of the green emission band, and therefore, further investigations need to clarify this point.

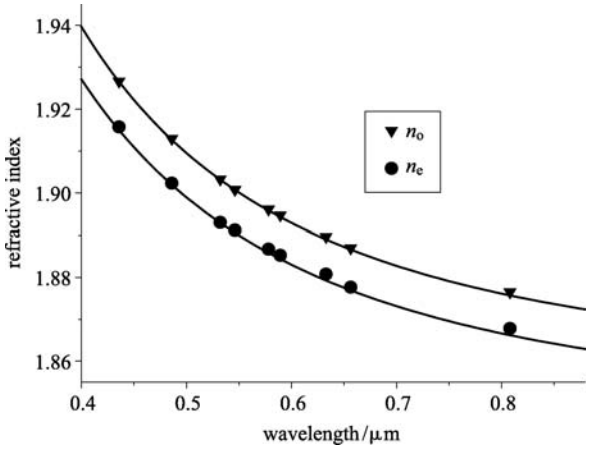

Figure 6 Dispersion of the refractive indices and calculated curves from the Sellmeir coefficients for $SrWO_4$.

5.2 Strontium tungstate containing rare-earth ions

The radii for eight coordinated Sr^{2+} and lanthanide ions are 1.26 nm and 0.98–1.16 nm, respectively [62]. When trivalent rare-earth ions are incorporated into the strontium tungstate lattice, they are expected to accommodate on the Sr^{2+} site with an S_4 site symmetry coordinated with eight oxygen atoms (Figure 8). In this case, the excess of charge is compensated by the incorporation of Na^+ or Nb^{5+} ions [63] present in the growth mixture or by the formation of cation vacancies. The charge compensation produces a slight difference in the spatial distribution of oxygen ions around the lanthanide ions and then the local fields acting on them, which will lead to the inhomogeneous broadening of the absorption and emission spectra even at low temperature [64].

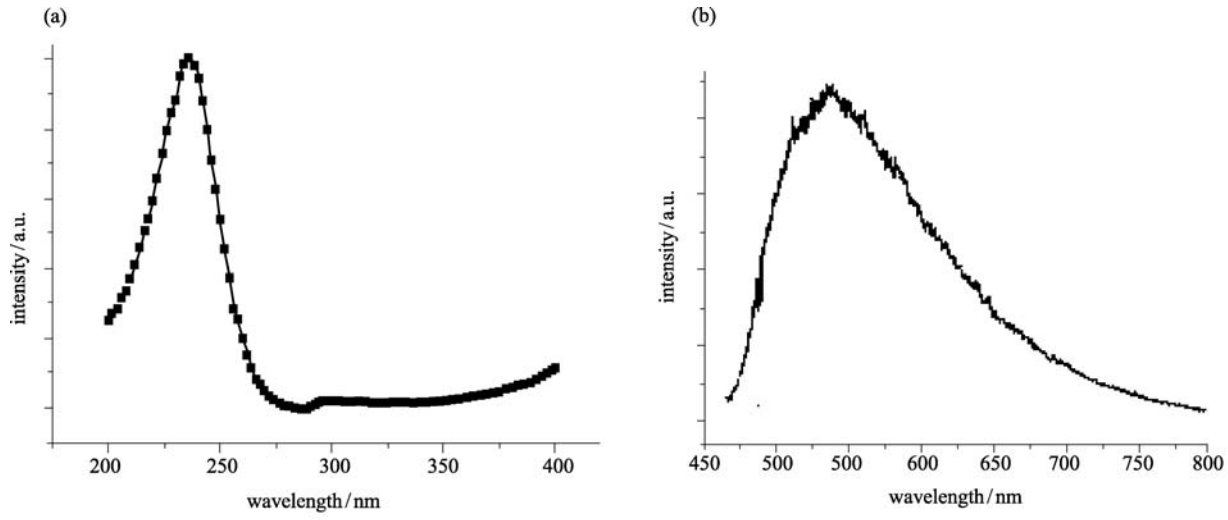

Figure 7 (a) Room temperature excitation and (b) emission spectra of neat $SrWO_4$. Figure reproduced from Refs. [47,50].

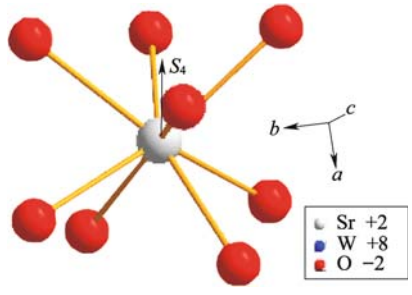

Figure 8 The coordination environment of Sr^{2+} in strontium tungstate crystal.

A series of lanthanide ions have been doped into the strontium tungstate lattice, and they have been subjected to detailed optical spectroscopy, Judd-Oflet calculation, and crystal field simulation [64–71]. We will not go into the details of these studies, but only summarize the optical spectra (Figures 9–14) and obtained parameters of strontium tungstate containing rare-earths ions herein.

The room temperature absorption spectra of strontium tungstate containing rare-earth ions are shown in Figures 9–14. Each spectrum displays the distinct fine structure of the dopant rare-earth ion, suggesting that rare-earth ions enter the Sr^{2+} site of the crystal lattice. Since the concentrations of rare-earth ions have been measured, the absorption spectra can be employed to perform the Judd-Ofelt calculation to theoretically determine the Judd-Ofelt parameters, radiative probabilities, and branching ratios [72,73]. The calculated intensity parameters for each rare-earth ion in strontium tungstate crystal are tabulated in Table 3.

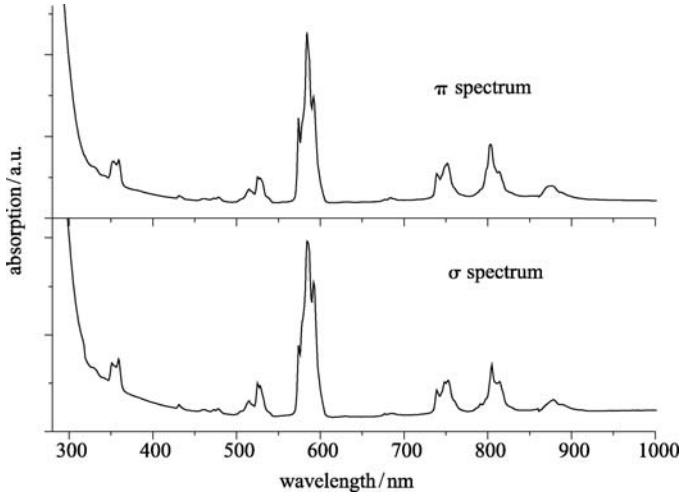

Figure 9 Room temperature polarized absorption spectra of Nd^{3+}:$SrWO_4$ crystal. Figure reproduced from Ref. [66].

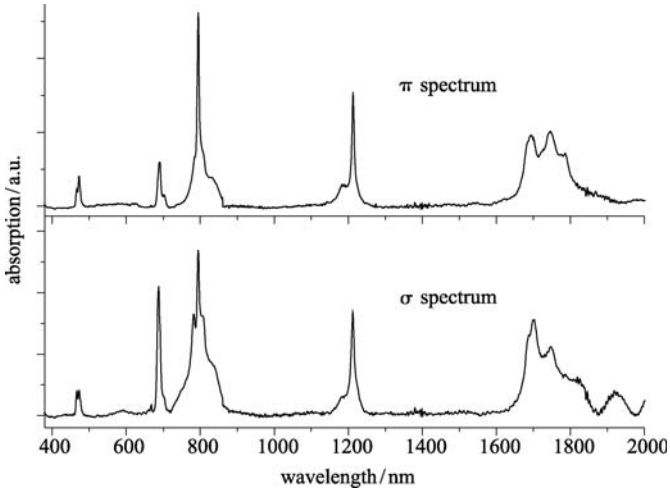

Figure 10 Room temperature polarized absorption spectra of Tm^{3+}:$SrWO_4$ crystal. Figure reproduced from Ref. [65].

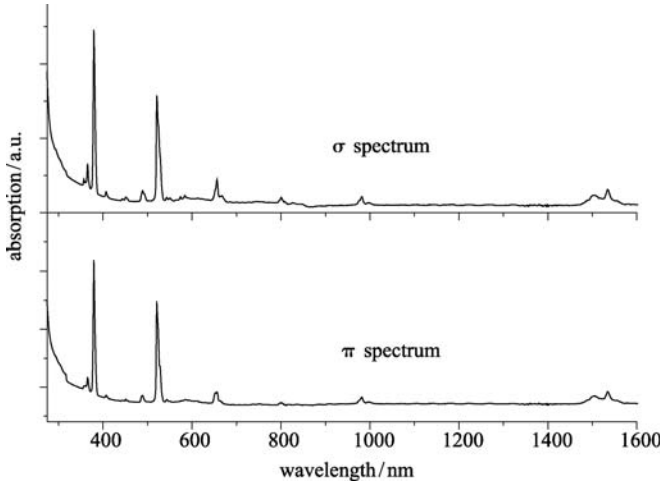

Figure 11 Room temperature polarized absorption spectra of Er^{3+}:$SrWO_4$ crystal. Figure reproduced from Ref. [67].

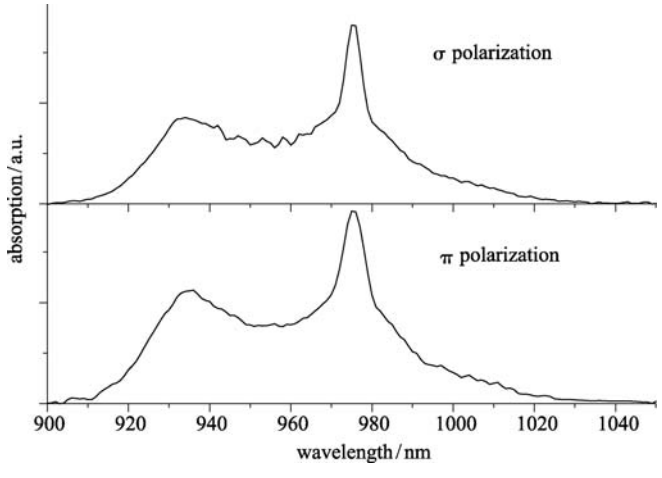

Figure 12 Room temperature polarized absorption spectra of Yb^{3+}:$SrWO_4$ crystal. Figure reproduced from Ref. [68].

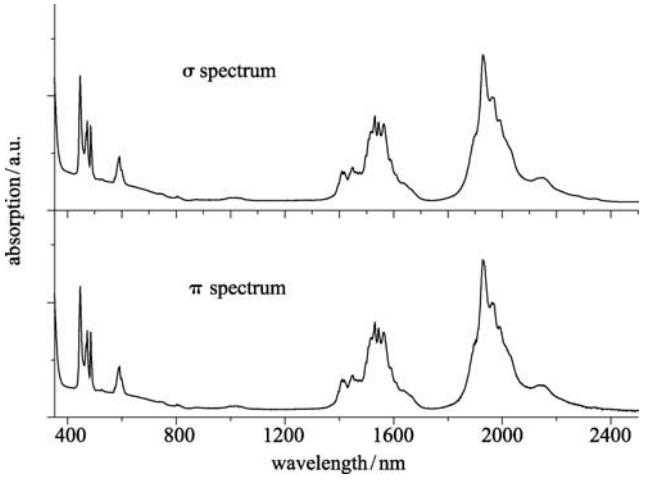

Figure 13 Room temperature polarized absorption spectra of Pr^{3+}:$SrWO_4$ crystal. Figure reproduced from Ref. [70].

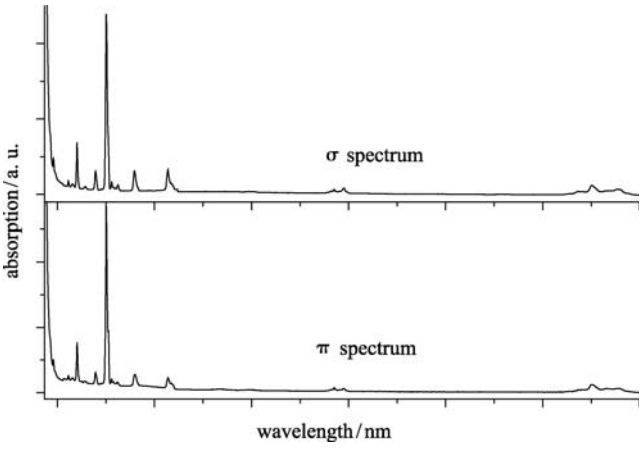

Figure 14 Room temperature polarized absorption spectra of Ho^{3+}:$SrWO_4$ crystal. Figure reproduced from Ref. [69].

Table 3 The calculated Judd-Ofelt parameters in strontium tungstate containing rare-earth ions. Ω_t ($t = 2$, 4, and 6) are in the unit of 10^{-20} cm^2

Ln^{3+}	Ω_2	Ω_4	Ω_6	Ref.
Nd	12.49	5.72	4.39	[64]
	12.39	2.48	2.80	[66]
Tm	7.41	0.25	1.71	[65]
Pr	14.9	1.8	6.8	[70]
Ho	12.21	3.95	1.23	[69]

6 Laser properties

The stimulated Raman scattering (SRS) phenomenon was firstly observed by Woodbury and Ng in 1962 [74]. Since then, the research on this phenomenon has received considerable attention due to its wide applications not only in macroscopic behavior of materials under high laser power radiation but also in microscopic optics of individual atoms, ions, and molecules.

It is well known that totally symmetric vibrations of molecules or groups in a crystal can produce the most intense Raman lines [75]. Accordingly, nitrates, tungstates, carbonates, and molybdate are the most promising crystals for efficient SRS. The crystal structure of strontium tungstate has been well introduced in the previous section. This unique structure allows the introduction of impurity ions and the usage of these crystals as matrices for laser active elements with nonlinear self-conversion of radiation to a new spectral range [75]. In recent years, there are lots of studies on SRS of neat and rare-earth ions doped strontium tungstate [76–93]. The most attractive one is Nd^{3+}-doped $SrWO_4$ crystal.

Firstly, we will review the recent investigations on the self-SRS in Nd^{3+}:$SrWO_4$. Figure 15 shows the dependencies of the laser output energy (1.06 μm) versus the flash lamp energy for 78%, 56%, and 37% reflectivity output couplers in Nd^{3+}:$SrWO_4$ [63]. The active element is 4 mm in diameter and 47 mm in length without antireflection coatings. The crystal was tested at 10 Hz pulse repetition rate in linear cavity 100 mm long, composed with two flat mirrors. In this experiment, the output energy of the first Stokes laser at 1.18 μm of the $^4F_{3/2} \rightarrow {}^4I_{11/2}$ transition is 3 mJ, and the pulse duration is 12 ns.

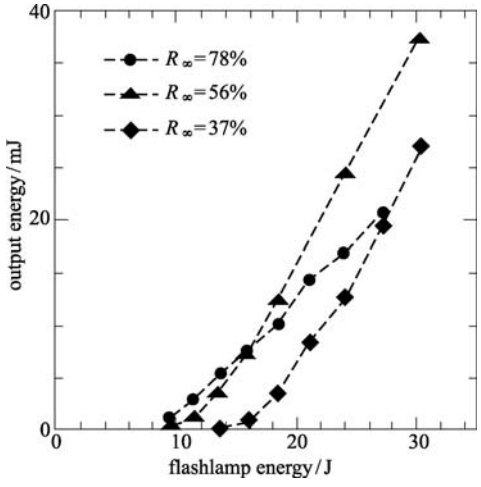

Figure 15 The dependencies of the laser output energy (1.06 μm) versus the flash lamp energy for 78%, 56%, and 37% reflectivity output couplers in Nd^{3+}:$SrWO_4$. Figure reproduced from Ref. [63].

We have demonstrated the Raman laser at 1.171 μm and 1.517 μm with self-frequency conversion in $SrWO_4$:Nd^{3+} crystal [87]. The $SrWO_4$:Nd^{3+} sample was 4 mm in diameter and 4.1 cm in length. It was oriented along the *a*-axis. The sample was excited near 750 nm with a Laser Analytical Systems dye laser pumped by a pulsed frequency-doubled Nd:YAG laser from BM Industries (duration of pulses: 8 ns). Laser pulses were generated at 1057 nm, and SRS self-frequency conversion pulses were observed at 1171 nm (Stokes 1) in *c*-polarization for the $^4F_{3/2} \rightarrow {}^4I_{11/2}$ transition. The energies of the laser and the Stokes 1 SRS pulses were measured with a Molectron pyrometer through adequate interference filters and are represented in Figure 16 versus the pump power. The threshold of the Stokes 1 SRS is close to the one of the laser, and the maximum Stokes 1 SRS conversion was 1.8%.

The laser tests of self-stimulated Raman scattering of the $^4F_{3/2} \rightarrow {}^4I_{13/2}$ laser channel were also investigated. The cavity was constituted of an entrance plane mirror with high transmission at 1060 and 750 nm and high reflection at 1331 nm, and an output concave mirror having 15 cm radius of curvature, high reflection at 1060 nm and 5% transmission at 1520 nm. Laser pulses were observed at 1331 nm and SRS

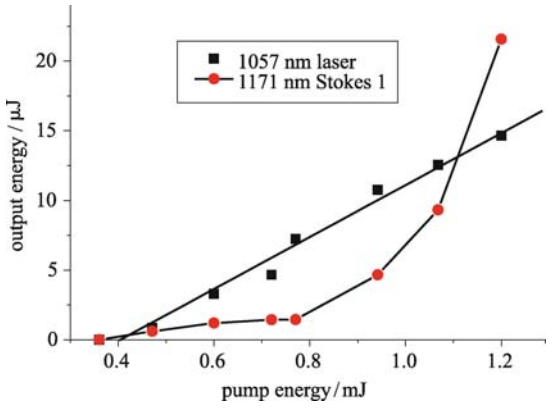

Figure 16 Laser and Stokes 1 output power from self-stimulated Raman scattering of the $^4F_{3/2} \rightarrow {}^4I_{11/2}$ laser transition. Figure reproduced from Ref. [87].

Stokes 1 at 1517 nm, both in *c*-polarization. Laser and Stokes 1 output power from self-stimulated Raman scattering of the $^4F_{3/2} \rightarrow {}^4I_{13/2}$ laser transition are shown in Figure 17. The maximum conversion efficiency of the pump towards the Stokes 1 SRS was 0.4%.

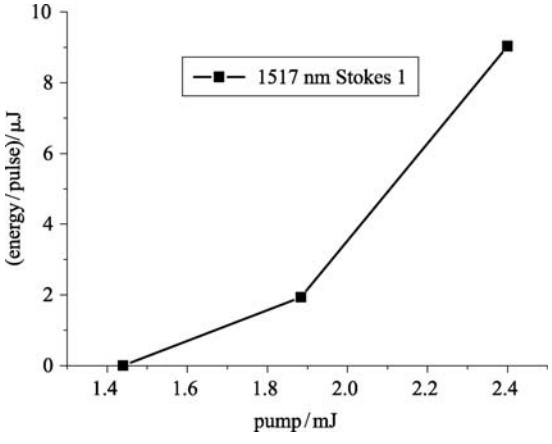

Figure 17 Laser and Stokes 1 output power from self-stimulated Raman scattering of the $^4F_{3/2} \rightarrow {}^4I_{13/2}$ laser transition. Figure reproduced from Ref. [87].

The parameters of the first stokes Raman laser of Nd^{3+}:$SrWO_4$ were summarized in Table 4.

Table 4 Parameters of the first Stokes self-SRS laser of Nd^{3+}:$SrWO_4$

Nd^{3+}	pumping wavelength/nm	first Stokes/ nm	pulse duration/ ns	pulse energy/ mJ	H/%	Ref.
0.33 wt.%	750	1171	22		1.8	[87]
0.5 at.%	752	1170	2.9	4.5	0.4	[79]
1 wt.%	752	1181	12	3	—	[63]
0.5 at.%	752	1170	2.9	1.23	—	[85,92]

Other work mainly focused on the Q-switch Nd:YAG/$SrWO_4$ or Nd:YVO_4/$SrWO_4$ Raman laser [79,80,85,88,92–94]. Ding et al. demonstrated the highly efficient frequency conversion of 50% from 1064 nm to the first-Stokes 1180 nm of nanosecond pump pulses in $SrWO_4$ crystal [90]. Chen et al. reported a highly efficient end-diode-pumped actively Q-switched Nd:YAG/$SrWO_4$ intracavity Raman laser with a conversion efficiency of 23.8% [88]. More recently, they demonstrated a diode side-pumped actively Q-switched Nd:YAG/$SrWO_4$ Raman laser with high average output power of 10.5 W at 1180 nm [80].

7 Conclusions

The recent advances in the fabrication, spectroscopy, and laser property of neat and rare-earth ions doped strontium tungstate have been reviewed. This material can be either grown into bulk crystals or fabricated into particles and films with the control of preparation conditions. The characteristic features of the absorption spectra of each rare-earth ion confirmed that the dopant accommodated on the strontium site in this host. The incorporation of rare-earth ions into strontium tungstate crystal provides a facile way to generate lasers in new wavelength regions, which has been proved by the recent demonstrations on the output of SRS lasers, especially in Nd^{3+}-doped $SrWO_4$. We hope that this review may spark the interest of scientists in this exciting field.

Acknowledgements This work was supported by the Doctoral Science Foundation of Linyi Normal University (BS08006). G. H. J. acknowledges the receipt of a postgraduate studentship administered by City University of Hong Kong.

Aixiang WANG is an associate professor in College of Chemistry and Chemical Engineering at Linyi Normal University. She received her Ph. D. degree in June 2008 from Northwest Normal University. Her research interests mainly include material synthesis and spectral analysis. She has published more than 30 papers in domestic and international academic journals.

Guohua JIA received his Ph.D. degree in July 2009 from City University of Hong Kong. Since then, he has worked as a postdoctoral fellow with Prof. Peter A. Tanner. Dr. Jia has published more than 60 papers in SCI journals. His main research interests cover the synthesis and solid-state spectroscopy of inorganic materials containing lanthanides, as well as optical properties of semiconductors.

References

1. Guermen, E.; Daniels, E.; King, J. S., *J. Chem. Phys*. **1971**, *55*, 1093–1097
2. Errandonea, D.; Pellicer-Porres, J.; Manjón, F. J.; Segura, A ; Ferrer-Roca, Ch.; Kumar, R. S.; Tschauner, O.; Rodríguez-Hernández, P.; et al., *Phys. Rev. B* **2005**, *72*, 174106
3. Rodríguez-Hernández, P,; López-Solano, J.; Radescu, S.; Mujica, A.; Muñoz, A.; Errandonea, D.; Pellicer-Porres, J.; Segura, A.; et al., *J. Phys. Chem. Solid*. **2006**, *67*, 2164–2171
4. Manjón, F. J.; Errandonea, D.; López-Solano, J.; Rodríguez-Hernández, P.; Radescu, S.; Mujica, A.; Muñoz, A.; Garro, N.; et al., *Phys. Stat. Sol. B* **2007**, *244*, 295–302
5. Errandonea, D., *Europhys. Lett.* **2007**, *77*, 56001
6. Packter, A.; Roy, B. N., *J. Crystal Growth* **1973**, *18*, 86–93
7. Jia, G. H.; Tu, C. Y.; You, Z. Y.; Li, J. F.; Zhu, Z. J.; Wang, Y.; Wu, B. C., *J. Crystal Growth* **2004**, *273*, 220–225
8. Ling, Z. C.; Xia, H. R.; Ran, D. G.; Liu, F. Q.; Sun, S. Q.; Fan, J. D.; Zhang, H. J.; Wang, J. Y.; et al., *Chem. Phys. Lett*. **2006**, *426*, 85–89
9. Fan, J. D.; Zhang, H. J.; Wang, J. Y.; Jiang, M. H.; Boughton, R. I.; Ran, D. G.; Sun, S. Q.; Xia. H. R., *J. Appl. Phys*. **2006**, *100*, 063513
10. Qi, X. D.; Luo, Z. D.; Liang, J. K., *J. Crystal Growth* **2000**, *246*, 363–366
11. Sczancoski, J. C.; Cavalcante, L. S.; Joya, M. R.; Espinosa, J. W. M.; Pizani, P. S; Varelab, J. A.; Longob, E., *J. Colloid Interface Sci*. **2009**, *330*, 227–236
12. Chen, Z.; Gong, Q.; Zhu, J.; Yuan, Y. P.; Qian, L. W.; Qian, X. F., *Mater. Res. Bull*. **2009**, *44*, 45–50
13. Thongtem, T.; Phuruangrat, A.; Thongtem, S., *Appl. Surface Sci*. **2008**, *254*, 7581–7585
14. Thongtem, T.; Phuruangrat, A.; Thongtem, S., *Current Appl. Phys*. **2008**, *8*, 189–197
15. Chen, D.; Ye, J. H., *Adv. Funct. Mater*. **2008**, *18*, 1922–1928
16. Dong, F. Q.; Wu, Q. S.; Sun, D. M.; Ding, Y. P., *J. Mater. Sci*. **2008**, *43*, 641–644
17. Joseph, S.; George, T.; George, K. C.; Sunny, A. T.; Mathew, S., *Nanotechnology and Its Applications, First Sharjah International Conference*; **2007**, p 95–99
18. Zhao, X. F.; Cheung, T. L. Y.; Zhao, X. T.; Ng, D. H. L., *J. Am. Ceram. Soc*. **2006**, *89*, 2960–2963
19. Thangadurai, V.; Knittlmayer, C.; Weppner, W., *Mater. Sci. Eng. B* **2004**, *106*, 228–233
20. Thongtem, T.; Phuruangrat, A.; Thongtem, S., *Appl. Surface Sci*. **2008**, *254*, 7765–769
21. Chen, Y.; Wu, Q. S.; Ding, Y. P., *NANO: Brief Rep. Rev*. **2007**, *2*, 195–199
22. Sun, L. N.; Guo, Q. R.; Wu, X. L.; Luo, S. J.; Pan, W. L.; Huang, K. L.; Lu, J. F.; Ren, L.; et al., *J. Phys. Chem. C* **2007**, *111*, 532–537
23. Afanasiev, P., *Mater. Lett*. **2007**, *61*, 4622–4626.
24. Gao, D. J.; Xiao, D. Q.; Jin, Y. X.; Bi, J.; Yu, P.; Lai, X., *J. Funct. Mater*. **2005**, *5*, 711–714
25. An, H. N.; Yang, Z. N.; Xiao, D. Q.; Yu, P.; Liu, Z. Q.; Chen, L. P.; Huang, X.; Wang, H., *J. Synth. Cryst*. **2007**, *5*, 1056–1061
26. Maurera, M. A. M. A.; Souza, A. G.; Soledade, L. E. B.; Pontes, F. M.; Longo, E.; Leite, E. R.; Varela, J. A., *Mater. Lett*. **2004**, *58*, 727–732
27. Pontes, F. M.; Galhiane, M. S.; Santos, L. S.; Petit, L. A.; Kataoka, F. P.; Mabuchi, G. H.; Longo, E.; Zampieri, M.; et al., *J. Alloys Compd*. **2009**, *477*, 608–615
28. Cui, C. H.; Bi, J.; Gao, D. J. J., *Crystal Grwoth* **2008**, *310*, 4385–4389
29. Orhan, E.; Anicete-Santos, M.; Maurera, M. A. M. A.; Pontes, F. M.; Paiva-Santos, C. O.; Souza, A. G.; Varela, J. A.; Pizani, P. S.; et al., *Chem. Phys*. **2005**, *312*, 1–9
30. Huang, J. Y.; Jia, Q. X., *Thin Solid Films*, **2003**, *444*, 95–98
31. Choosuwan, H.; Guo, R.; Bhalla, A. S.; Balachandran, U., *J. Appl. Phys*. **2002**, *91*, 5051
32. Carvajal, J. J.; Sole, R.; Gavalda, J.; Massons, J.; Diaz, F.; Aguilo, M., *Chem. Matt*. **2003**, *15*, 2730–2736
33. Mu, G. G.; Zhan, Y. L., *Optics* (in Chinese); People's Education Press: Beijing, 1978
34. Born, M.; Wolf, E., *Principles of Optics*; Pergamon: Oxford, 1975
35. Treadaway, M. J.; Powell, R. C., *J. Chem. Phys*. **1974**, *61*, 4003–4011
36. Blasse, G.; Schipper, W., *J. Phys. Stat. Sol. A* **1974**, *25*, K163–168
37. Groenink, J. A.; Blasse, G. J., *Solid State Chem*. **1980**, *32*, 9–20
38. Canham, L. T., *Appl. Phys. Lett*. **1990**, *57*, 1046–1048
39. Lecoq, P.; Dafinei, I.; Auffray, E.; Schneegans, M.; Korzhik, M. V.; Missevitch, O. V.; Pavlenko, V. B.; Fedorov, A. A.; et al., *Nucl. Instrum. Meth. A* **1995**, *365*, 291–298
40. Korzhik, M. V.; Pavlenko, V. B.; Timoschenko, T. N.; Katchanov, V. A.; Singovskii, A. V.; Annenkov, A. N.; Ligun, V. A.; Solskii, I. M.; et al., *Phys. Status Solidi A* **1996**, *154*, 779–788
41. Sinelnikov, B. M.; Sokolenko, E. V.; Zvekov, V. Y., *Inorg. Mater*. **1996**, *32*, 999–1001
42. Sokolenko, E. V.; Zhukovskii, V. M.; Buyanova, E. S.; Krasnobaev, Y. A., *Inorg. Mater*. **1998**, *34*, 499–502
43. Annenkov, A. A.; Korzhik, M. V.; Lecoq, P., *Nucl. Instrum. Method. A* **2002**, *490*, 30–50
44. Shi, C.; Wei, Y.; Yang, X.; Zhou, D.; Guo, C.; Liao, J.; Tang, H., *Chem. Phys. Lett*. **2000**, *328*, 1–4
45. Qi, Z.; Shi, C.; Zhou, D.; Tang, H.; Liu, T.; Hu, T., *Physica B* **2001**, *307*, 45–50
46. Chen, Y.; Shi, C.; Hu, G., *J. Appl. Phys*. **2000**, *87*, 1503–1506
47. Huang, Y.; Zhu, W.; Feng, X., *J. Electron Spectrosc. Relat. Phenom*. **2003**, *133*, 39–45
48. Cho, W. S.; Yashima, M.; Kawihana, M.; Kudo, A.; Sakata, T.; Yoshimura, M., *J. Am. Ceram. Soc*. **1995**, *78*, 3110–3112
49. Wu, S. Y.; Dong, H. N.; Yan, W. Z.; Gao, X. N., *Phys. Stat. Sol. B* **2004**, *241*, 1073–1077
50. Anicete-Santos, M.; Lima, R. C.; Orhan, M. A. M. A.; Simoes, L. G. P.; Souza, G.; Pizani, P. S.; Leite, E. R.; Varela, J. A.; et al.,

Compu. Aid. Mater. Design **2005**, *12*, 111–119

51. Anicete-Santos, M.; Picon, F. C.; Escote, M. T.; Leite, E. R.; Pizani, P. S.; Varala, J. A.; Longo, E., *Appl. Phys. Lett*. **2006**, *88*, 211913
52. Arora, S. K.; Chudasama, B., *Cryst. Res. Technol*. **2006**, *41*, 1089–1095
53. Jia, R. P.; Zhang, G. X.; Wu, Q. S., *Appl. Phys. Lett*. **2006**, *89*, 043112
54. Chen, L. P.; Gao, Y. H., *Mater. Res. Bull*. **2007**, *42*, 1823–1830
55. Kovács, L.; Péter, Á.; Ivleva, L. I.; Baraldi, A.; Capelletti, R., *Phys. Stat. Sol. C* **2007**, *4*, 856–859
56. Longo, V. M.; Orhan, E.; Cavalcante, L. S.; Porto, S. L.; Espinosa, J. W. M.; Varela, J. A.; Longo, E., *Chem. Phys*. **2007**, *334*, 180–188
57. Lacomba-Perales, R.; Ruiz-Fuertes, J.; Errandonea, D.; Martinez-Garcia, D.; Segura, A., *Europhys. Lett.* **2008**, *83*, 37002
58. Porto, S. L.; Longo, E.; Pizani, P. S.; Boschi, T. M.; Simoes, L. G P.; Lima, S. J. G.; Ferreira, J. M.; Soledade, L. E. B.; et al. *J. Solid State Chem*. **2008**, *181*, 1876–1881
59. Zhang, G. X.; Jia, R. P.; Wu, Q. S., *Mater. Sci. Eng. B* **2006**, *128*, 254–259
60. Blasse, G., *Structure Bonding* **1980**, *42*, 1–41
61. Butler, P. H., *Point Group Symmetry Application: Methods and Tables*; Plenum: New York, 1981
62. Shannon, R. D., *Act. Cryst. A* **1976**, *32*, 751–767
63. Ivleva, L. I.; Basiev, T. T.; Boronina, I. S.; Zverev, P. G.; Osiko, V. V.; Polozkov, N. M., *Opt. Mater*. **2003**, *23*, 439–442
64. Cornacchia, F.; Toncelli, A.; Tonelli, M.; Cavalli, E.; Bovero, E.; Magnani, N. J., *Phys.*: *Condens. Matt*. **2004**, *16*, 6867–6876
65. Jia, G. H.; Tu, C. Y.; You, Z. Y.; Li, J. F.; Zhu, Z. J.; Wu, B. C., *Solid State Commu*. **2005**, *134*, 583–588
66. Jia, G.; Tu, C.; Brenier, A.; You, Z.; Li, J.; Zhu, Z.; Wang, Y.; Wu, B., *Appl. Phys. B: Lasers Opt*. **2005**, *81*, 627–632
67. Jia, G. H.; Tu, C. Y.; You, Z. Y.; Li, J. F.; Zhu, Z. J.; Yan, W.; Wu, B. C., *J. Appl. Phys*. **2005**, *98*, 093525
68. Jia, G. H.; Li, J. F.; Zhu, Z. J.; You, Z. Y.; Yan, W.; Wu, B. C.; Tu, C. Y., *J. Alloy. Compd*. **2007**, *436*, 341–344
69. Li, J. F.; Jia, G. H.; Zhu, Z. J.; You, Z. Y.; Yan, W.; Wu, B. C.; Tu, C. Y., *J. Phys. D: Appl. Phys*. **2007**, *40*, 1902–1905
70. Jia, G.; Wang. H.; Lu, X.; You, Z.; Li, J.; Zhu, Z.; Tu, C., *Appl. Phys. B: Lasers Opt*. **2008**, *90*, 497–502
71. Rivera-López, F.; Martín, I. R.; da Silva, I.; González-Silgo, C.; Rodríguez-Mendoza, U. R.; Lavín, V.; Lahoz, F.; Díaz-González, S. M.; et al., *High Pressure Res*. **2006**, *26*, 355–359
72. Judd, B. R., *Phys. Rev*. **1962**, *127*, 750–761
73. Ofelt, G. S. J., *Chem. Phys*. **1962**, *37*, 511–520
74. Woodbury, E. J.; Ng, W. K., *Proc. IIRE* **1962**, *50*, 2367–2380
75. Eckhardt, G., *IEEE J. Quant. Elect*. **1966**, *2*, 1–8
76. Voronina, I. S.; Ivleva, L. I.; Basiev, T. T.; Zverev, P. G.; Polozkov, N. M., *J. Optoelect. Adv. Mater*. **2003**, *5*, 887–892
77. Kaminskii, A. A.; Bagaev, S. N.; Ueda, K.; Takaichi, K.; Eichler, H., *J. Crystallo. Report* **2002**, *47*, 653–657
78. Achima, A.; Gheorghe, L.; Lupei, V.; Lupei, A.; Cheorche, C.; Stoicescu, C., *J. Optoelect. Adv. Mater*. **2008**, *6*, 1353–1356
79. Basiev, T. T.; Doroshenko, M. E.; Ivleva, L. I.; Osiko, V. V.; Kosmyna, M. B.; Komar, V. K.; Jelinkova, J. S. H., *Quant. Elect*. **2006**, *36*, 720–726
80. Chen, X. H.; Zhang, X. Y.; Wang, Q. P.; Li, P.; Li, S. T.; Cong, Z. H.; Liu, Z. J.; Fan, S. Z.; et al., *J. Laser Phys. Lett*. **2009**, *6*, 363–366
81. Hu, D. W.; Wang, Z. P.; Zhang, H. J.; Xu, X. G.; Wang, J. Y.; Shao, Z. S., *Chin. Phys. Lett*. **2006**, *23*, 2766–2768
82. Jelinkova, H.; Sulc, J.; Basiev, T. T.; Zverev, P. G.; Kravtsov, S. V., *Laser Phys. Lett*. **2005**, *2*, 4–11
83. Lupei, A.; Lupei, V.; Gheorghe, C.; Gheorghe, L.; Achim, A., *J. Appl. Phys*. **2008**, *104*, 083102
84. Mlyczak, J.; Kopczyski, K.; Mierczyk, Z., *Opt. Appl*. **2008**, *4*, 657–668
85. Sulc, J.; Jelinkova, H.; Basiev, T. T.; Doroschenko, M. E.; Ivleva, L. I.; Osiko, V. V.; Zverev, P. G., *Opt. Mater*. **2007**, *30*, 195–197
86. Wang. Z. P.; Hu, D. W.; Zhang, H. J.; Xu, X. G.; Wang, J. Y.; Shao, Z. S., *J. Inorg. Mater*. **2009**, *24*, 563–566
87. Brenier, A.; Jia, G. H.; Tu, C. Y., *J. Phys.*: *Condens. Matt*. **2004**, *16*, 9103–9108
88. Chen, X. H.; Zhang, X. Y.; Wang, Q. P.; Li, P.; Li, S.T.; Cong, Z. H.; Jia, G. H.; Tu, C. Y., *Opt. Lett*. **2008**, *33*, 705–707
89. Basiev, T. T.; Sobol, A. A.; Voroko, Y. K.; Zverev, P. G., *Opt. Mater*. **2000**, *15*, 205–216
90. Ding, S. H.; Zhang, X. Y.; Wang, Q. P.; Su, F. F.; Li, S. T.; Fan, S. Z.; Liu, Z. J.; Chang, J.; et al., *IEEE J. Quant. Elect*. **2006**, *42*, 78–84
91. Cong, Z. H.; Zhang, X. Y.; Wang, Q. P.; Liu, Z. J.; Li,S. T.; Chen, X. H.; Zhang, X. L.; Fan, S. Z.; et al., *Opt. Lett*. **2009**, *34*, 2610–2612
92. Jelinkova, H.; Sulc, J.; Doroschenko, M. E.; Skornyakov, V. V.; Kravtsov, S. B.; Basiev, T. T.; Zverev, P. G., *Proc. SPIE* **2004**, *5460*, 99–109
93. Sulc, J.; Jelinkova, H.; Basiev, T. T.; Doroschenko, M. E.; Ivleva, L. I.; Osiko, V. V.; Zverev, P. G., *Proc. SPIE* **2006**, *6100*, 61000Z
94. Fan, Y. X.; Lin, Y.; Duan, Y. H.; Wang, Q.; Fan, L.; Wang, H.T.; Jia, G. H.; Tu, C. Y., *Appl. Phys. B: Lasers Opt*. **2008**, *93*, 327–330